Environmental Science Advances

ROYAL SOCIETY OF CHEMISTRY

PAPER

View Article Online
View Journal | View Issue

Cite this: *Environ. Sci.: Adv.*, 2026, **5**, 1406

Deciphering the plastisphere nexus in biological wastewater treatment: distinct microbial colonization on biodegradable and conventional microplastics

Gaurav Bhardwaj,[a] Lachi Wankhede,[a] Ratul Kumar Das,[a] Ahmed Eldyasti,[a] Ahmed Koubaa[b] and Satinder Kaur Brar *[a]

Microplastics (MPs) are ubiquitous in wastewater treatment plants (WWTPs), where their persistent presence has been shown to alter treatment performance and microbial community structure. However, existing studies largely emphasize bulk system responses, while the underlying mechanisms, including biofilm formation on MP surfaces, remain insufficiently characterized. In particular, the extent to which microbial colonization on MP surfaces is selective, polymer-dependent and evolves over time under WWTP conditions remains poorly resolved. To address this gap, this study systematically compares plastisphere development on four conventional polymers, polyethylene (PE), polypropylene (PP), polystyrene (PS), and polyethylene terephthalate (PET), and a biodegradable polymer, polylactic acid (PLA) under sequencing batch reactor (SBR) conditions. Biofilm biomass increased up to 5-fold, with PLA exhibiting the highest accumulation (OD_{595nm} = 1.067; $p < 0.05$), substantially exceeding conventional MPs. Intrinsic polymer properties shaped microbial colonization through selective enrichment on MP surfaces. While PLA supported a transient peak in community diversity and selectively enriched plastic-degrading taxa such as *Comamonas* (~16–25%), continuous hydrolytic oxidation and surface pitting prevented stable long-term community retention. In contrast, conventional MPs converged toward low-diversity biofilms dominated by pioneer genera including *Raoultella* (~80–90%). Among conventional MPs, PS exhibited the strongest divergence at biofilm maturity, functioning as a persistent reservoir for ESKAPE pathogens. PS specifically enriched *Acinetobacter* (8.17 log2-fold-change), demonstrating that while biodegradable surfaces promote robust general microbial growth, the structural permanence of conventional microplastics provides a more selective and reliable substrate for long-term pathogen persistence. Together, these findings highlight polymer-specific plastisphere development as a key biological pathway governing MP transformation and microbial partitioning in WWTPs, with implications for MP fate and sludge-associated microbial risks.

Received 12th January 2026
Accepted 7th April 2026

DOI: 10.1039/d6va00023a

rsc.li/esadvances

Environmental significance

Microplastics are pervasive in wastewater treatment plants, where they interact with microbial communities and influence the dynamics of contaminants and pathogens. While their impacts on treatment performance have been widely reported, the underlying mechanisms governing microplastic–microbe interactions remain poorly understood. This knowledge gap limits our ability to accurately assess microplastics fate, associated risks, and potential mitigation strategies in engineered water systems. This study demonstrates that biofilm formation on microplastics is polymer-specific, with biodegradable plastics selectively enriching plastic-degrading microorganisms, while certain conventional plastics preferentially accumulate opportunistic pathogens. These findings reveal biofilm-mediated pathways through which microplastics are transformed and biologically partitioned in wastewater treatment, with important implications for microplastic persistence, pathogen retention in sludge, and downstream environmental exposure.

1 Introduction

Microplastics (MPs) are plastic particles smaller than 5 mm that arise as primary pellets or as secondary fragments from the degradation of larger plastic debris.[1] MPs are a global concern, particularly due to their presence and persistence in aquatic environments.[2] In these settings, microbes rapidly colonize MP

[a]*Civil Engineering Department, Lassonde School of Engineering, York University, North York, Ontario M3J1P3, Canada. E-mail: satinder.brar@lassonde.yorku.ca*

[b]*Forest Research Institute (Institut de recherche sur les forêts–IRF), Université du Québec en Abitibi–Témiscamingue (UQAT), 445 Boul. de l'Université, Rouyn-Noranda J9X 5E4, QC, Canada*

surfaces and form the plastisphere, a structured biofilm embedded in extracellular polymeric substances (EPS).[3] The EPS matrix supports adhesion, protection from stressors, and cell–cell communication through quorum signalling.[4] MP-associated biofilms can enrich opportunistic pathogens and antibiotic resistance genes (ARGs), while EPS can promote horizontal gene transfer (HGT) by concentrating extracellular DNA and bringing cells into close contact.[5,6] The small size, low density, and hydrophobicity of MPs favour long-range transport and persistence, which may amplify the spread of pathogens and ARGs with implications for ecosystems and human health.[7,8]

Biofilm formation on MPs proceeds through distinct stages: initial colonization, reversible adhesion transitioning to irreversible attachment, growth, and dispersion.[9] MP properties and environmental conditions govern these dynamics alongside exposure duration.[10,11] Hydrophobicity and surface energy guide the initial adhesion, while roughness, charge, and weathering-driven oxidation stabilize the EPS matrix.[12] Concurrent gradients in nutrients, oxygen, and shear drive succession from early colonizers to mature consortia.[13] Co-occurring stressors, such as antibiotics, metals, and organic micropollutants, also impose selection that further structures the plastisphere.[14]

Previous plastisphere research has largely centred on freshwater and marine systems,[15,16] while wastewater treatment plants (WWTPs) are comparatively overlooked despite acting as major conduits to receiving waters, with individual facilities discharging up to 5×10^7 MPs per day.[17] This effluent load represents roughly the residual 1% of incoming MPs; the remaining 99% are retained and partitioned to sewage sludge, where 1500–170,000 MPs per kg dry weight have been reported.[18] This accumulation is significant because MPs interact with microorganisms and can release or carry toxic compounds, which may affect biological treatment processes. Consequently, most MP studies in WWTPs have emphasized treatment efficiency and sludge microbiology.[19,20] Yet this focus often overlooks the underlying mechanism in biological wastewater treatment units, the biofilm formation on MP surfaces. The dense microbial consortia, continuous substrate supply, controlled hydrodynamics, and strong nutrient and oxygen gradients within these treatment units collectively create near-optimal conditions favouring biofilm formation on MPs. This underrepresentation constitutes a prominent research gap: understanding the plastisphere within biological treatment units of WWTPs. Closing this knowledge gap is essential for understanding how the biological processes in WWTPs influence the selection of microorganisms specific to MPs, pathogen enrichment, and MP weathering processes.

Previous studies of the wastewater plastisphere have shown that MP-attached microbial communities differ from those in bulk sludge, forming a distinct plastisphere.[21] However, the extent to which this plastisphere varies by polymer type remains largely unexplored in WWTPs. Feng *et al.* (2023) compared polyethylene terephthalate (PET), polystyrene (PS), polycarbonate (PC), and polyethylene (PE) in the aerobic and anaerobic tanks of a WWTP, but did not include any biodegradable plastics.[22] Although biodegradable polymers such as polylactic acid (PLA) accumulate in WWTPs and often exhibit higher adsorption affinity and act as stronger microbial and chemical carriers than non-biodegradable MPs,[23] direct comparisons between biodegradable and non-biodegradable MPs remain scarce. A few comparisons of conventional *versus* biodegradable MPs exist; for instance, Martínez-Campos *et al.* evaluated four conventional and three biodegradable polymers but focused only on the first 48 hours of colonization, leaving later stages and succession unaddressed.[24] A direct comparison of biofilm formation on conventional *versus* biodegradable MPs within wastewater biological treatment units remains understudied across both early and long-term colonization.

To the best of our knowledge, it will be the first comprehensive reporting on the side-by-side plastisphere comparison of five distinct MP polymers, four conventional (PE, PP, PS, PET) and one biodegradable (PLA), in sequencing batch reactors (SBRs) over 30 days, resolving both early and long-term colonization across defined biofilm stages. By using environmentally relevant MP concentrations and identical test conditions for all MPs, this work overcomes the inconsistency and limited comparability of previous studies. Accordingly, the objectives focus on three main parts. The first objective is to quantify and compare differential biofilm formation on conventional *versus* biodegradable MPs using identical SBRs over time. The characterization of bacterial diversity and community structure of MP-attached consortia across biofilm stages using 16S rRNA gene amplicon sequencing has been studied and presented as the second objective of the study. The final objective is to systematically evaluate the colonization and enrichment of pathogenic bacteria together with evidence for microbial degradation and associated physicochemical weathering of MPs in WWTPs.

2 Materials and methods

2.1. Microplastics, experimental setup, and operation

Five model MPs with distinct physicochemical properties and environmental relevance were selected, including PLA (Ingeo™ 2003D, NatureWorks), PET (Arnite® A06700, DSM), PS (STYRON 6860, Dow), PP (HG455FB, Borealis), and PE (Purell GA7760, LyondellBasell), and were used in pellet form with the largest dimension of 3–4 mm. Before use, pellets were rinsed with distilled water, sterilized in 70% ethanol for 30 min, rinsed with sterile phosphate-buffered saline (PBS), and stored in sterile containers at room temperature. During start-up, 200 MPs were added per reactor, corresponding to 100 MPs per g VSS, as a single dose under aseptic conditions to ensure uniform exposure while limiting aggregation.

Reactor configuration and operational conditions followed an established SBR protocol described previously.[25] Briefly, eighteen identical cylindrical glass SBRs (1 L total volume; 0.40 L working volume; inner diameter 10.0 cm; total height 18 cm) were set up to run six conditions in triplicate, five receiving a single MP type and one serving as an MP-free control. Reactors were maintained at an ambient temperature of 25 ± 1 °C with orbital mixing at 180 rpm on 12 h cycles comprising 6 h aerobic

and 4 h anoxic phases, with the remaining time allocated to fill, settle, and decant. Synthetic wastewater was fed at the start of each cycle (SI, Text S1), and 0.20 L was decanted at the end, yielding a hydraulic retention time of 24 h.

2.2. Analytical methods

2.2.1. Sampling design. Sampling was conducted on days 3, 15, and 30 per reactor replicate. These time points correspond to early colonization and transition to irreversible attachment (day 3), growth and maturation (day 15), and late maturation with initial dispersion (day 30). A 30-day incubation represents 3-fold of the steady-state profile, and it is sufficient for robust biofilm formation on MPs, consistent with prior studies.[26]

At each time point, fifty MPs were aseptically removed per reactor for analysis. Low-density MPs (PE and PP) floating on the surface were directly picked using sterile forceps, while denser MPs (PS, PET, and PLA) were scooped from the reactor bottom and then retrieved with forceps. The remaining MPs were left *in situ* for continued exposure. Sludge samples (2 mL) were collected concurrently from the MP-free control reactor to characterize the suspended microbial community.

2.2.2. Biofilm assessment

2.2.2.1. Crystal violet assay. Biofilm biomass on MPs was quantified by crystal violet staining.[27] Ten MPs per sample were rinsed three times with sterile water to remove loosely attached cells and air-dried for 45 min at room temperature. MPs were stained with 1% (w/v) crystal violet for 45 min, washed three times with sterile water, and air-dried for 45 min. Bound dye was solubilized in 1.0 mL of 95% (v/v) ethanol for 15 min, and the eluate was transferred to a 96-well plate. Absorbance at 595 nm was measured using a Synergy HT microplate reader (BioTek, Vermont, USA) with Gen5 software.

2.2.2.2. Scanning electron microscopy (SEM). Biofilm morphology on MPs was characterized by SEM (Tescan VEGA). Samples were rinsed with 0.1 M PBS and fixed in 2.5% glutaraldehyde for 12 h at 4 °C. Fixed samples were dehydrated through graded cold ethanol solutions (30, 50, 70, 90, and 100% v/v; 10 min each), mounted on aluminium stubs with carbon tape, sputter-coated with platinum using a Desktop V thin film deposition system, and imaged at different magnification.

2.2.3. DNA extraction and bacterial community analysis. Genomic DNA was extracted from detached MP biofilms using the DNA Kit (GenBio Systems, Inc., Canada) following the manufacturer's protocol. Yields from individual replicates were insufficient for library preparation. Therefore, DNA from the three reactor replicates per polymer per time point was pooled in equal mass before sequencing. DNA purity and concentration were then assessed with a NanoDrop Lite spectrophotometer (Thermo Scientific, USA). The V4 hypervariable region of the 16S rRNA gene was amplified by PCR using the primer pair 515F (GTGCCAGCMGCCGCGGTAA) and 806R (GGACTACNVGGGTWTCTAAT). Subsequent library preparation, purification, and amplicon sequencing on an Illumina platform were performed at the McMaster Genomics Facility, Faculty of Health Sciences, McMaster University, Hamilton, Ontario, Canada. Raw reads were processed with DADA2 package within the R software environment for quality filtering, error correction, dereplication, paired-read merging, chimera removal, and inference of amplicon sequence variants for downstream community analysis.[28]

2.2.4. Microplastic characterization. Surface morphology after 30 days of incubation was examined by SEM (Tescan VEGA). Pristine MPs served as controls. Representative particles were mounted on aluminum stubs with carbon tape, sputter-coated with platinum, and imaged at various magnifications. Attenuated Total Reflectance-Fourier Transform Infrared (ATR-FTIR) spectra were collected on a Bruker Alpha-P over 400–4000 cm^{-1} with 16 scans at 4 cm^{-1} resolution for pristine and 30-day exposed MPs to assess changes in functional groups.

2.2.5. Statistical analysis. All statistical analyses and visualizations were performed in OriginPro 2025 (OriginLab, Northampton, USA). Differences in biofilm biomass across MP type and time were tested by two-way repeated-measures analysis of variance (ANOVA), followed by Tukey's post hoc comparisons; $p < 0.05$ was considered significant. Microbial community analyses were conducted in Microbiome Analyst (version 2.0).[29] To compare bacterial community compositions on different MP surfaces and assess the factors influencing these communities, Alpha diversity was computed using Chao1, Shannon, and Simpson indices. Beta diversity was assessed using Bray–Curtis dissimilarities and visualized by principal coordinates analysis (PCoA).

3 Results and discussion

3.1. Temporal dynamics of microplastic-associated biofilm

Fig. 1(a) shows microbial biomass attached to MPs at days 3, 15, and 30, with a representative SEM image of PLA at day 30 in Fig. 1(b). Across time, attached biomass increased significantly from day 3, day 15 to day 30 for all polymers by two-way repeated-measures ANOVA ($p < 0.05$). Over 30 days, biofilm levels rose by approximately 3 to 6-fold across polymers, with PLA showing the steepest trajectory. These temporal patterns were consistent with previous reports of significant biomass increases over 30-day incubations in wastewater matrices.[30]

Day 3 represented early colonization, with measurable but statistically indistinguishable biomass across polymers as shown in Fig. 1(a). Biomass values ranged from approximately 0.07 to 0.18, with PLA highest at 0.182 ± 0.029. These small differences aligned with the reversible-to-irreversible transition, during which conditioning films dominated adhesion.

By day 15, representing the growth and maturation stage, biomass had increased on all polymers (Fig. 1(a)). PLA showed significantly higher biofilm than the other MPs, reaching an OD of 0.478 ± 0.053, approximately 1.6–2.2 times greater than that of the conventional polymers. Among the conventional polymers, PS (0.290 ± 0.041) was numerically higher than PET (0.213 ± 0.029), although this difference was not significant. This trend aligned with Feng *et al.*, who observed more pronounced increases in PS surface roughness than in PET after 15-day incubation in aerobic reactors.[22] Taken together, the day 15 hierarchy likely reflected surface-governed processes. PLA underwent hydrolytic and oxidative modification that increased

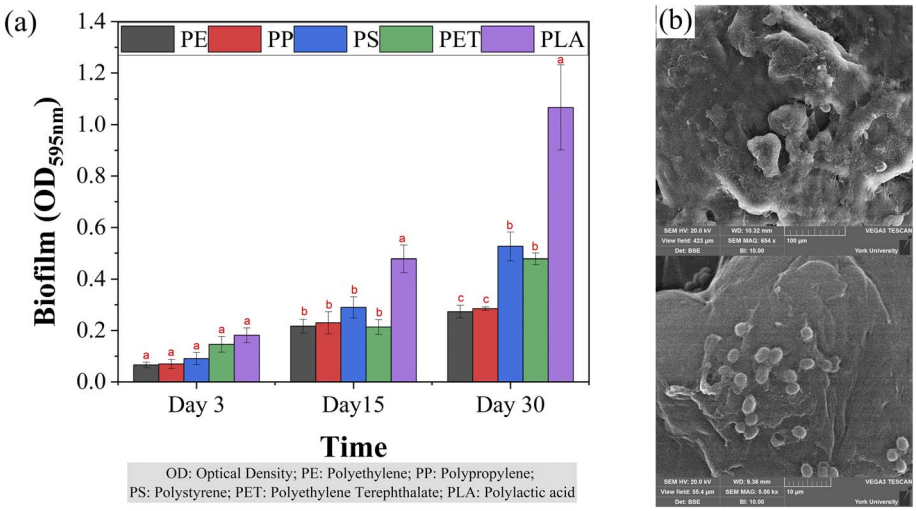

Fig. 1 (a) Temporal dynamics of biofilm formation on polyethylene (PE), polypropylene (PP), polystyrene (PS), polyethylene terephthalate (PET), and polylactic acid (PLA) MPs at days 3, 15, and 30. Bars represent mean ± SD from triplicate reactors. Different letters above bars within the same time point indicate significant differences among polymer types based on two-way repeated-measures ANOVA followed by post hoc testing ($p < 0.05$). (b) Representative SEM micrograph of PLA at day 30 showing coccus microcolonies embedded in the EPS matrix.

surface polarity and micro-roughness, which enhanced EPS anchoring. PS and PET showed intermediate accumulation because of their higher surface energies; PET also presented a polar, oxidizable surface. In contrast, the low-surface-energy polyolefins remained the least colonized.

By day 30, attached biomass had increased further for all polymers and resolved into three distinct tiers in Fig. 1(a): PLA was highest, PS and PET were intermediate, and PE and PP were lowest. PLA reached an OD of 1.067 ± 0.165, approximately twice that of PS and PET and nearly four times that of PE and PP. The PLA micrograph revealed coccus microcolonies embedded within a dense EPS matrix, highlighting extensive biofilm accumulation on PLA (Fig. 1(b)). Representative SEM images detailing the distinct biofilm morphologies for the other MPs are shown in Fig. 2.

The intermediate responses of PS and PET were consistent with their surface characteristics. PS is an aromatic polymer with relatively high surface energy that promotes adhesion, and PET is a polar, oxidizable polyester that supports EPS retention. Both outperformed the low-surface-energy polyolefins under identical conditions but remained below PLA. These outcomes aligned with prior evidence that biodegradable polymers aged more rapidly. Wang *et al.* (2025) reported larger 30-day increases in FTIR carbonyl index for PLA than for PE and PET, indicating greater oxidative weathering of biodegradable MPs, which increases surface polarity and micro-roughness and helps explain the highest biomass observed on PLA.[30]

Biofilm formation on MPs in SBRs followed the expected colonization stages: attachment, growth, and maturation, with biomass steadily increasing over 30 days. Polymer type strongly influenced these dynamics: biodegradable PLA fostered more robust colonization than conventional polyolefins and polyesters. These insights are crucial for understanding the fate of MPs in WWTPs and for optimizing treatment processes to mitigate their environmental impact.

3.2. Bacterial community ecology of MP-associated biofilms

3.2.1. Bacterial diversity. 16S rRNA gene amplicon sequencing profiled bacterial communities on MPs after 3, 15, and 30 days of incubation in SBRs. A total of 1 842 646 reads were obtained from 15 pooled libraries (5 polymers × 3 sampling days). Alpha diversity, quantifying within-sample diversity, and Beta diversity, capturing between-sample differences, were assessed as shown in Fig. 3.

Alpha diversity was evaluated using Chao1 (richness), Simpson (evenness), and Shannon (richness and evenness) indices (Fig. 3(1)). The control sludge exhibited a distinct diversity profile compared to the MP-associated biofilms. Throughout the study, it maintained a consistently lower species richness (Chao1). However, its overall diversity (Shannon and Simpson indices) remained relatively stable. Consequently, by day 30, the control sludge surpassed most MP communities in overall diversity as the plastispheres matured and specialized. This disparity highlighted the intense selective enrichment occurring on MP surfaces.

Across polymers, overall diversity and evenness, represented by the Shannon and Simpson indices, were highest at day 3, declined at day 15, and partially recovered by day 30. Conversely, species richness measured by the Chao1 index generally increased from day 3 to day 15 across most MPs, indicating an accumulation of rare taxa as the biofilms developed. Taken together, the indices indicated relatively even communities during early colonization followed by a mid-stage consolidation. This consolidation was driven by dominance of a few surface-adapted taxa that lowered overall evenness despite the concurrent increase in species richness. A later re-balancing occurred as the communities mature. This temporal sequence was consistent with prior work; for example, Lai *et al.* (2022) observed a diversity peak around day 6, followed by a decline by day 16 during maturation.[31]

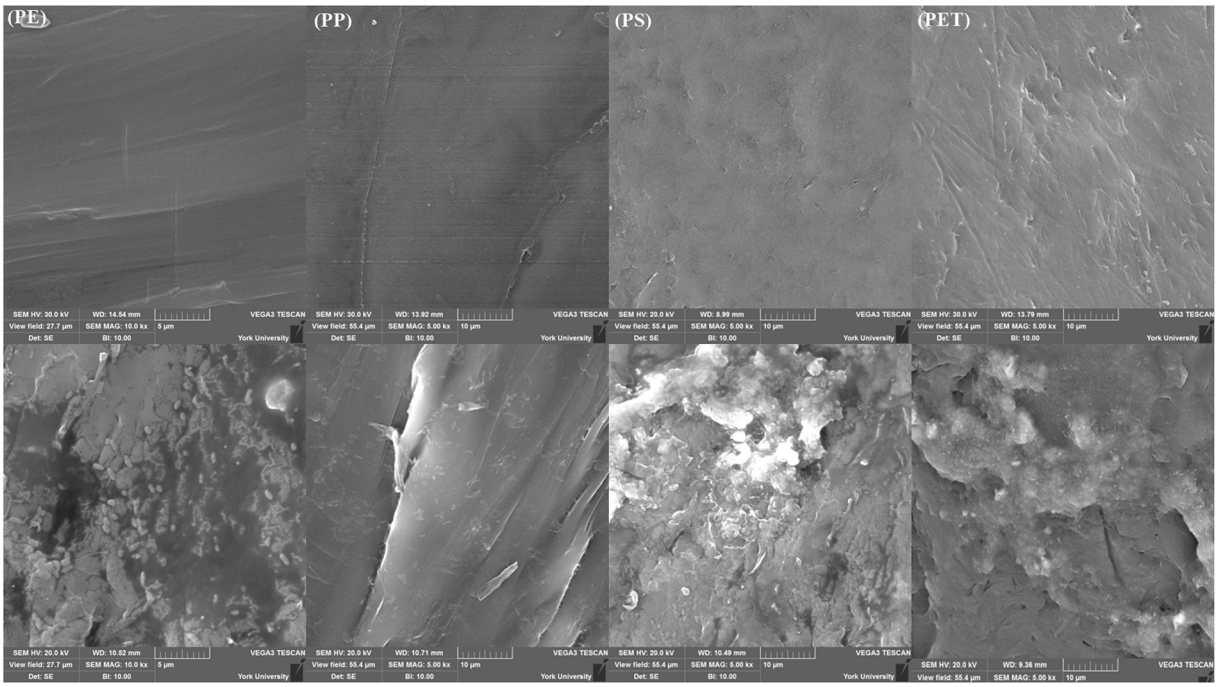

Fig. 2 Representative SEM images MP-associated biofilms before and after 30-day incubation in SBRs.

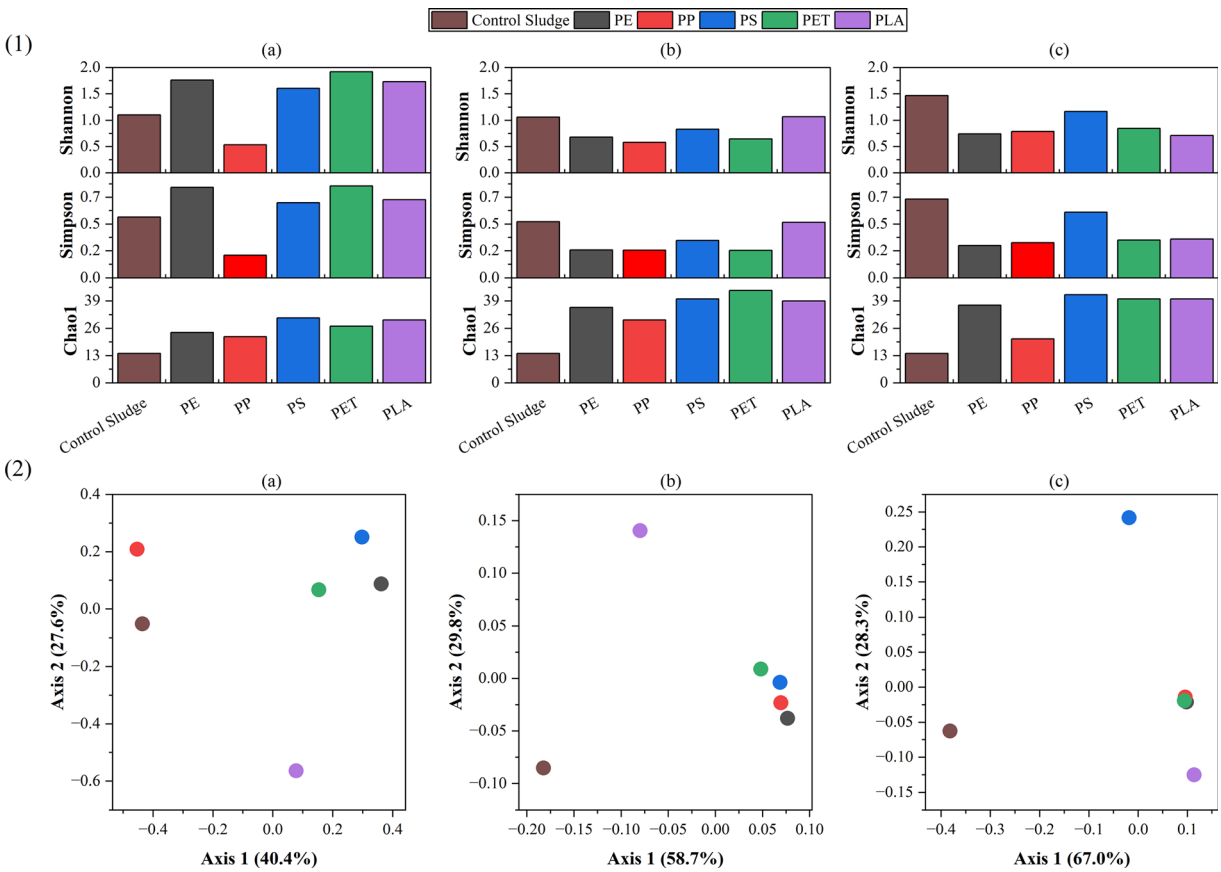

Fig. 3 Bacterial community diversity in microplastic-associated biofilms and sludge across time. (1) Alpha diversity for control, PE, PP, PS, PET, and PLA at: (a) day 3, (b) day 15, and (c) day 30 is shown as bar graphs for Shannon, Simpson, and Chao1. (2) Beta diversity by PCoA of Bray–Curtis dissimilarities at (a) day 3, (b) day 15, and (c) day 30.

Polymer type governed the internal diversity dynamics within the MP-associated biofilms (Fig. 3(1)). For the biodegradable polymer PLA, within-sample diversity peaked at day 15, where it supported the highest diversity among all MPs, before experiencing a sharp decline by day 30. This temporal pattern builds upon previous reports, such as those by Martínez-Campos *et al.*, who observed highly diverse bacterial assemblages on biodegradable MPs compared to conventional ones.[24] However, the observed trends indicate that this elevated diversity on PLA may represent a transient phase during mid-stage colonization rather than a permanent characteristic of the mature biofilm. Among the conventional, non-biodegradable polymers, distinct patterns emerged. By day 30, diversity within the PS-associated biofilm developed to be the highest across all tested MPs. In contrast, the polyolefin PP maintained the lowest diversity throughout the entire 30-day incubation. Meanwhile, PE and the polyester PET exhibited higher initial diversity that subsequently decreased as the plastispheres matured. Ultimately, the unique diversity dynamics observed on each polymer type indicate strong surface-specific selection. This is consistent with literature establishing that microplastic properties, rather than simple bulk biomass, are the primary drivers of plastisphere composition.[32]

Beta diversity was visualized using Principal Coordinate Analysis (PCoA) based on Bray–Curtis dissimilarities (Fig. 3(2)). Across all time points at days 3, 15, and 30, the most prominent trend was the distinct and consistent separation of the control sludge from the microplastic-associated biofilms. The control sludge occupied an isolated position in the ordination space, confirming that the microplastics did not merely recruit a random subset of the surrounding microbial community. Instead, the solid polymer surfaces exerted a strong selective pressure that drove the assembly of a highly specialized plastisphere, a phenomenon consistent with previous studies demonstrating that microplastics host microbial assemblages inherently distinct from their surrounding bulk environments.[21] Axis 1 and Axis 2 represented the dominant gradients in community dissimilarity, expressed as variance explained. The magnitude of this compositional divergence between the suspended sludge and the surface-attached communities became more pronounced as the biofilms matured, with the variance explained by the primary gradient on Axis 1 increasing from 40.4% at day 3 to 67.0% by day 30.

During early colonization (day 3), the ordination revealed a wide dispersion among the plastispheres, driven by two primary gradients in community dissimilarity (Axis 1 = 40.4%, Axis 2 = 27.6%) (Fig. 3(2a)). Unlike the later stages of incubation where certain communities began to converge, the day 3 plastispheres were highly distinct from one another, scattering widely across the ordination space. This broad distribution suggests that multiple factors, such as polymer composition, surface chemistry (surface charge, hydrophobicity), and physical characteristics (roughness, topography), acted synergistically during early biofilm formation, rather than a single dominant property dictating the community structure. Notably, PP occupied a distinct position, segregating entirely from other polyolefins like PE along the primary axis. This early divergence is consistent with reports that pristine PP exhibits greater surface roughness and microtopography, which can alter conditioning-film adsorption and initial microbial attachment, thereby yielding divergent early community structures.[33] Overall, these distinct spatial patterns confirm that rapid, polymer-specific selective colonization occurs within the first three days of exposure.

During the growth and maturation phase (days 15 and 30), distinct community dynamics emerged within the plastisphere (Fig. 3(2b and c)). At day 15, the communities on the conventional polymers began to group together, whereas the biodegradable PLA diverged distinctly along Axis 2. By day 30, the community structures on PE, PP, and PET converged into a highly compact cluster. This convergence suggests that the development of mature biofilms and extensive surface conditioning ultimately diminished the impact of their initial surface chemistry differences. In contrast, PLA and PS remained highly isolated from this central polyolefin and polyester cluster by day 30, separating in opposite directions along Axis 2. In contrast, PLA and PS remained highly isolated from this central polyolefin and polyester cluster by day 30, separating in opposite directions along Axis 2. The persistent spatial offset of PLA aligns with biodegradability-driven hydrolytic aging, which alters surface polarity and micro-roughness to support a distinct community. Meanwhile, the distinct trajectory of the PS biofilm reflects the unique selective pressure by its higher surface energy and aromatic structure. Overall, these ordination patterns evidence that while certain conventional polymers host convergent communities upon maturation, distinct material properties such as biodegradability or aromaticity continue to drive highly specialized selective colonization over time.

3.2.2. Taxonomic structure and composition. The control sludge community was co-dominated by Proteobacteria (47.8%) and Bacteroidota (36.5%), a profile typical of biological treatment systems. In contrast, a distinct plastisphere assembled rapidly on the MPs (Fig. 4). During early colonization (day 3), biofilms were mainly composed of Proteobacteria together with Actinobacteriota, approaching ~99% across polymers. This

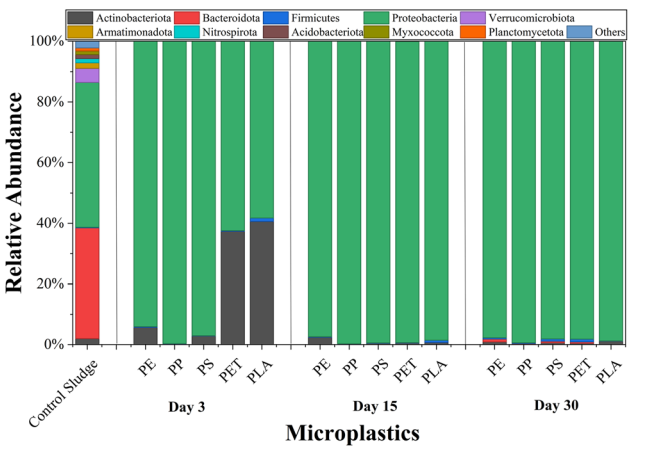

Fig. 4 Phylum-level community composition of MP-associated biofilms over time (3 d, 15 d, and 30 d).

represented a drastic shift from the control sludge, as Bacteroidota was nearly completely excluded from the early MP biofilms. Early polymer-specific colonization was evident: PET and PLA co-enriched Actinobacteriota to about 37–41%, representing a massive enrichment compared to its minor presence (2%) in the control sludge, consistent with higher diversity at this stage. Greater surface polarity, which promoted conditioning-film adsorption and cation bridging, likely contributed to these patterns. In contrast, polyolefins (PE, PP) and PS were nearly exclusively Proteobacteria, consistent with prior reports of Proteobacteria enrichment on polyolefin surfaces in MP-associated plastispheres within SBRs.[33]

Through growth and maturation (days 15 and 30), communities converged toward near-complete domination by Proteobacteria, accounting for ~99% of all MPs. Weak but reproducible residues persisted, with Bacteroidota more evident on PE, and PP, Firmicutes on PET, and Actinobacteriota on PLA. This rapid divergence from the planktonic baseline and the consolidation toward Proteobacteria over time indicated strong surface-mediated selective colonization on MPs driven by material properties such as surface energy, polarity, and biodegradability. These patterns were consistent with reports that Proteobacteria, Actinobacteriota, Bacteroidota, and Firmicutes were versatile biofilm formers frequently enriched on MPs, including plastic-degrading and pathogenic lineages.[34–36]

The distinctive bacterial compositions in the planktonic and MP-associated biofilms were more revealing at the genus level. For instance, planktonic sludge communities were dominated by *Dokdonella*, *Ferruginibacter*, *Zoogloea*, and the nitrifiers *Nitrosomonas* and *Nitrospira*, spanning roughly 1–18% each (Fig. 5). In contrast, MP-associated biofilms displayed a markedly different genus profile, emphasizing selective colonization on polymer surfaces (Fig. 5). MP biofilms were enriched in Enterobacterales (notably *Raoultella* and, to a lesser extent, *Klebsiella*), together with Betaproteobacteria such as *Comamonas* and *Bordetella*, and Actinobacteria including *Corynebacterium* and *Glutamicibacter*. This divergence from the planktonic communities highlighted the plastisphere as a distinct ecological niche shaped by polymer identity and exposure time.

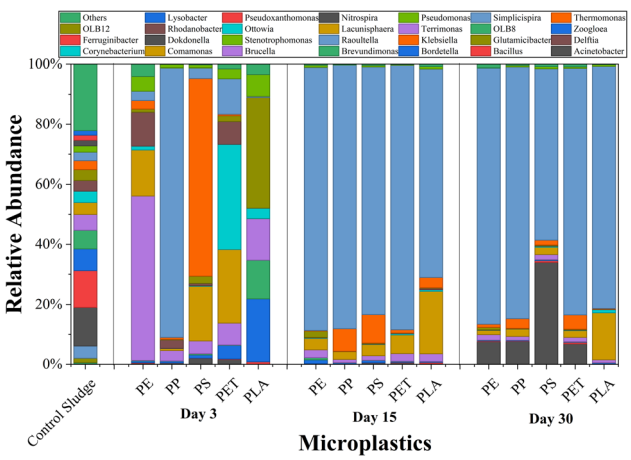

Fig. 5 Genus-level community composition of MP-associated biofilms over time (3 d, 15 d, and 30 d).

During early colonization (day 3), MP type selectively enriched distinct and diverse pioneer assemblages consistent with the observed diversity patterns and similar to the early colonization patterns reported by Martínez-Campos *et al.* (2021).[24] Hydrophobic and aromatic surfaces selected Enterobacterales-rich biofilms: PP was dominated by *Raoultella* (~90%), a prolific EPS producer and PS by *Klebsiella* (~66%), a recognized opportunistic pathogen, consistent with Kelly *et al.* (2021) and Bydalek *et al.* (2023), who identified *Klebsiella* as a key pathogenic taxon enriched on MPs in wastewater systems.[37,38] In contrast, PET and PLA surfaces were dominated by Actinobacteria-linked pioneers: PET hosted *Corynebacterium* (~35%) with *Comamonas* (~25%), and PLA enriched *Glutamicibacter* (~37%) with *Bordetella*. This aligns with Wilkes *et al.* (2024) and Jiao *et al.* (2024), who demonstrated *Comamonas* enrichment on PET,[39] and *Actinobacteria* dominated PLA biofilms.[40] These dominant taxa were known early colonizers in wastewater, capable of robust biofilm formation and metabolism of organics. The pattern indicated selective colonization driven by surface chemistry.

During the growth and maturation phase, by day 15, MP biofilms were dominated by *Raoultella* on all polymers (~69–88%), with *Klebsiella* as a secondary constituent, an EPS-rich consortium that explains the decline in evenness at this stage. This functional dominance aligns with findings by Pham *et al.* (2021) showing *Raoultella ornithinolytica* as a significantly enriched taxon on MPs with 1.6–3.3 enrichment indices.[41] Although distinct polymer signals persisted: on PLA, *Comamonas* comprised ~21%; on PS, *Klebsiella* remained at ~9–10%; on PET, minor *Actinobacteria* persisted.

By day 30, convergence remained, but polymer-linked features sharpened. *Raoultella* accounted for ~82–86% on PE, PP, PET, and PLA, accompanied by *Acinetobacter* at ~6–8%. PS showed the largest shift, with *Acinetobacter* rising to ~34% and co-dominating with *Raoultella*. Kim *et al.* (2025) also demonstrated that *Acinetobacter* sp. exhibits dose-dependent higher EPS production and enhanced biofilm formation on PS MPs.[42] PLA continued to show greater representation of *Comamonas* (~16%) than other MPs, supporting findings that biodegradable polymer biofilms retain distinct bacterial compositions with degradative capabilities. Functionally, these profiles indicated enrichment of opportunistic pathogen-associated genera on some materials by late maturation, particularly PS with high *Acinetobacter* and sustained Enterobacterales, whereas PLA supported a higher fraction of degraders such as *Comamonas*. This pattern supported surface-driven selection followed by functional convergence on EPS-producing Enterobacterales, with partial diversification at day 30 and persistent polymer-specific signatures in the mature plastisphere. This temporal succession pattern mirrors Tagg *et al.* (2022) findings showing polymer type shapes biofilm maturation and pathogen dynamics over extended incubation periods.[43]

3.2.3. Pathogen enrichment in MP-associated biofilms. MP-associated biofilms contained higher proportions of risk-relevant taxa than the control sludge, including groups of clinical and veterinary concern. This enrichment was quantified using $\log_2$-fold-change (LFC), which measures the binary

logarithm of the ratio between biofilm and control sludge relative abundances, with positive values indicating enrichment in MP-associated biofilms.[44] Among the dominant genera detected on MPs (Fig. 6), *Acinetobacter* and *Klebsiella*, members of the ESKAPE pathogens, exhibited substantial enrichment in the plastisphere, with maximum LFCs of 8.17 and 10.01, respectively. This reflects their well-known capacities for biofilm formation and antimicrobial resistance.[45] *Stenotrophomonas* and some *Corynebacterium*, recognized opportunistic pathogens in biological wastewater treatment systems that have also been implicated in fish disease in aquaculture settings,[46] showed maximum LFCs of 7.11 and 10.93, respectively, indicating their selective enrichment within MP biofilms.

Across time, pathogen-associated genera on MPs exhibited polymer-specific succession (Fig. 6). During early colonization (day 3), *Klebsiella* was heavily enriched on PS, showing a maximum LFC of 10.01, while PET strongly selected for *Corynebacterium*, reaching an LFC of 10.93. By day 15, the enrichment of *Klebsiella* declined on PS but increased on PET and PP to LFCs of 4.16 and 6.93, respectively, indicating material-specific selection during the biofilm growth phase. By day 30, *Acinetobacter* proliferated across all non-biodegradable conventional polymers, reaching LFCs between 5.85 and 8.17, with the highest enrichment observed on PS. Meanwhile, the initial strong enrichment of pioneer colonizers such as *Stenotrophomonas* and *Corynebacterium* generally contracted across most materials as the biofilms matured. Additionally, members of Nocardiaceae, frequently observed in treatment plants and including clinically significant *Nocardia* spp., were also enriched in MP biofilms[47] (SI, Fig. S1). These observations indicated that the plastisphere can act as a selective substrate for pathogen-associated lineages relative to the surrounding sludge.[48]

Taken together, the genus-level data showed polymer-dependent succession that concentrated opportunistic pathogens on specific MPs. PS carried consistently high burdens of these taxa throughout the maturation phase, whereas the biodegradable PLA exhibited the lowest overall enrichment by day 30. These taxa are likely embedded in EPS-rich matrices that promote adhesion, protect against oxidants, and concentrate extracellular DNA, thereby supporting persistence through biological treatment systems. Consequently, plastisphere-associated pathogens on selected polymers may be exported in effluents or sludges despite overall treatment reduction, posing risks to aquatic organisms and human health.[9]

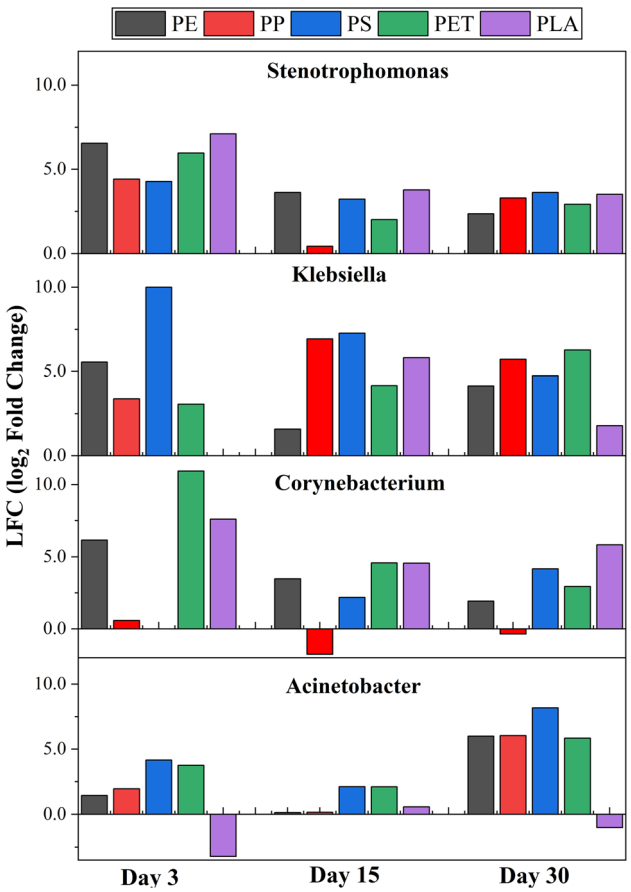

Fig. 6 Differential enrichment, expressed as log2 fold change (LFC), of genera comprising key pathogenic species observed in microplastic-associated biofilms at different incubation times (days 3, 15, and 30).

3.3. Physicochemical properties of MPs post-exposure

The selective enrichment of specific bacterial genera, including pathogens, capable of MP degradation in WWTPs, led to measurable property changes after 30 days in SBRs. PLA MPs exhibited clear signs of degradation, evidenced by distinct spectral alterations in the ATR-FTIR analysis, whereas PE, PP, PS, and PET remained largely stable (Fig. 7(a)).

The PLA spectra, as shown in Fig. 7(b), displayed a significant increase in the broad absorption band at 3295 cm^{-1}, which is characteristic of the O–H stretching vibration of hydroxyl end groups. This change strongly indicates the occurrence of hydrolytic chain scission of the ester bonds. Concurrently, the intensity of the characteristic aliphatic C–H stretching peaks at 2920 cm^{-1} (asymmetric C–H) and 2850 cm^{-1} (symmetric C–H) was reduced (Fig. 7(c)), reflecting the surface degradation and subsequent microbial uptake of the resulting short-chain molecules. Furthermore, the modest increases in carbonyl and C–O stretching bands between 1760 and 1080 cm^{-1} confirm the formation of other polar degradation products (such as carboxylic acid end groups), which collectively enhance the PLA surface wettability and correlate with the greater biomass accumulation observed on PLA MPs.[49]

Morphological analysis *via* SEM further corroborated the chemical changes, showing that PLA exhibited localized pitting, fissures, and etched domains, consistent with active microbial or enzymatic attack on the polymer matrix (SI, Fig. S2). In contrast, the PS MPs primarily displayed edge chipping, abrasion tracks, and minor surface scuffs, features characteristic of mechanical wear from mixing and shear against the reactor walls.[50] The lack of significant chemical change in conventional MPs indicated their resistance to substantial biofilm-mediated oxidation under the short-term SBR conditions. The distinct PLA morphology aligns with its surface oxidation and increased

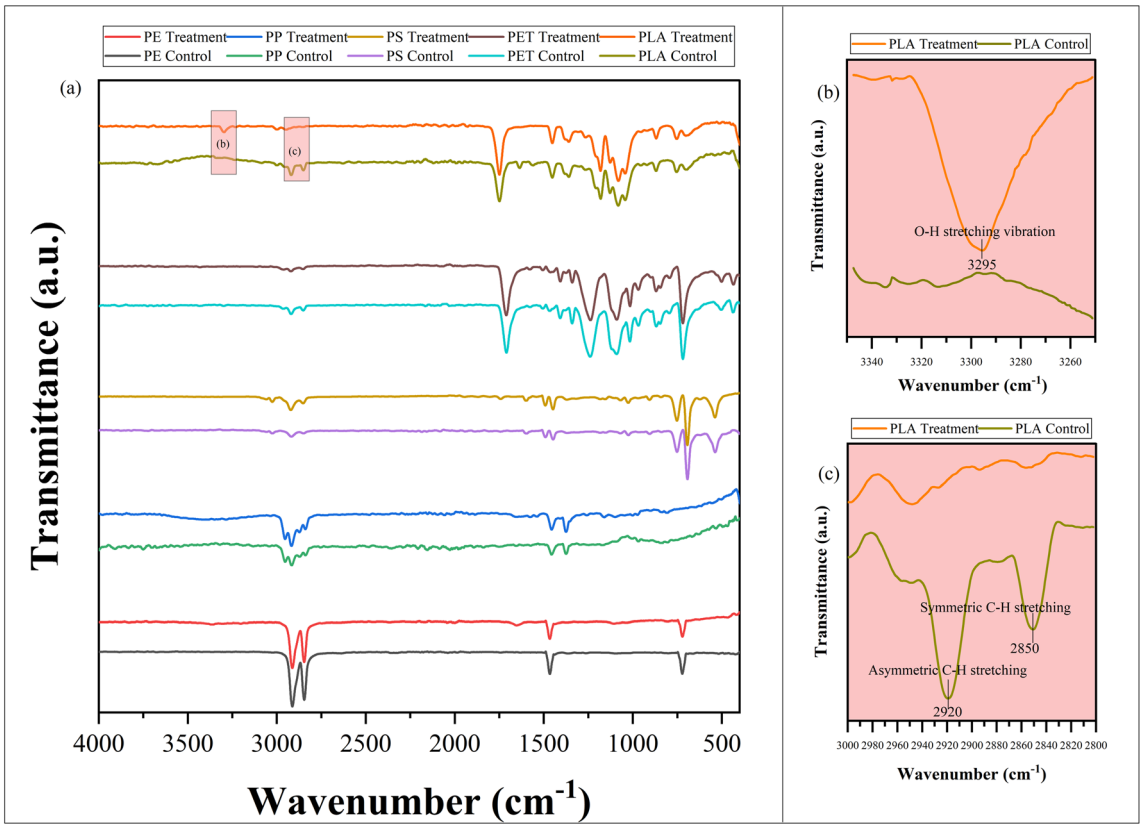

Fig. 7 Physicochemical changes of microplastics after 30 days in SBRs: (a) full ATR-FTIR spectra for PE, PP, PS, PET, and PLA before (control) and after exposure (treatment). Magnified views of the PLA spectra highlight (b) the O–H stretching vibration at 3295 cm^{-1} and (c) the asymmetric and symmetric C–H stretching at 2920 and 2850 cm^{-1}, respectively.

micro-roughness, which enhance wettability and provide additional anchoring sites for EPS. PS, meanwhile, developed microstructures that improve physical retention but lack clear FTIR-detectable oxidation. Together, the spectroscopic and microscopic evidence demonstrate polymer-specific weathering pathways over 30 days: PLA undergoes measurable chemical modification driven by microbial activity, whereas PS experiences predominantly mechanical alteration.

4 Conclusion

This study demonstrates that biofilm formation on MPs within biological wastewater treatment units is strongly governed by polymer-specific surface properties and biodegradability, resulting in distinct patterns of biomass accumulation and microbial community composition. Biofilm development followed material-dependent colonization trajectories, with biodegradable PLA consistently supporting the highest biofilm biomass. While PLA promoted a transient peak in microbial diversity and the selective enrichment of plastic-degrading taxa, such as *Comamonas*, coincided with pronounced hydrolytic aging and surface pitting, indicating that polymer degradability plays an important role in shaping later-stage plastisphere succession. Although, these dynamic surface alterations did not favour the long-term retention of opportunistic pathogens. In contrast, log_2-fold-change analysis revealed that highly stable conventional MPs, particularly PS, supported the highest and most persistent enrichment of specific risk-relevant taxa, including *Acinetobacter* and *Klebsiella*, by the mature biofilm stage. This distinction suggests that while biodegradable surfaces promote robust general microbial growth, the structural permanence of conventional polymers provides a more selective and reliable substrate for pathogen persistence within WWTPs.

Collectively, these findings reveal the plastisphere as a critical biological interface mediating MP–microbe interactions in wastewater treatment systems. While biofilm-associated processes may contribute to polymer surface modification and weathering, the extent to which such processes lead to fragmentation into nano plastics, and how intermediate degradation products (such as oligomers and monomers) from biodegradable polymers impact overall microbial health, remains unresolved. Future research should therefore prioritize long-term, multi-year *in situ* studies incorporating mixed polymer profiles to evaluate their combined impacts on sludge settling and the safety of final agricultural sludge reuse. Additionally, while pathogen retention was clearly demonstrated, the relative risk of antibiotic resistance gene (ARG) proliferation and spread *via* biodegradable *versus* conventional biofilms requires targeted, standardized investigation. Recognizing the dual role of MP-associated biofilms in both pathogen retention and polymer transformation is essential for developing

a comprehensive understanding of microplastic fate and behaviour within WWTPs.

Author contributions

Gaurav Bhardwaj: conceptualization, methodology, investigation, validation, formal analysis, writing – original draft, writing – review & editing. Lachi Wankhede: methodology, writing – review & editing. Ratul Kumar Das: writing – review & editing. Ahmed ElDyasti: supervision, writing – review & editing. Ahmed Koubaa: supervision, writing – review & editing. Satinder Brar: supervision, funding acquisition, writing – review & editing.

Conflicts of interest

There are no conflicts to declare.

Data availability

The sequence data generated and analyzed during the current study has been deposited in the Sequence Read Archive (SRA) maintained by the National centre for Biotechnology Information (NCBI) under the Bio Project ID PRJNA1436619 (Title: Microbial diversity in MP-associated biofilms in WWTPs). All other data supporting the findings of this study are available within the article and its corresponding supplementary information (SI) file. Supplementary information is available. See DOI: https://doi.org/10.1039/d6va00023a.

Acknowledgements

This research was funded by the Natural Sciences and Engineering Research Council (Discovery Grant 23451, NSERC Alliance Option-2 Grants, ALLRP 571066–21), "Microplastics in Sewage Sludge Exploration and Detection (MISSED)" project. We would also like to thank James and Joanne Love, Chair in Environmental Engineering and the Dahdaleh Institute for Global Health Research, for their financial support. The authors gratefully acknowledge Ripley's Aquarium for their knowledge mobilization efforts, the Surette Lab and the McMaster Genomics Facility for their sequencing assistance, and Dr Magdalena Jaklewicz at the York University Imaging Facility for her valuable help with the SEM analysis.

References

1 L. K. DH, G. Bhardwaj, R. Indhur, L. Wankhede, S. K. Brar and S. Kumari, Electrochemical approaches for detecting micro and nano-plastics in different environmental matrices, *Int. J. Electrochem. Sci.*, 2025, **20**, 101182.
2 J. Li, H. Liu and J. Paul Chen, Microplastics in freshwater systems: A review on occurrence, environmental effects, and methods for microplastics detection, *Water Res.*, 2018, **137**, 362–374.
3 E. R. Zettler, T. J. Mincer and L. A. Amaral-Zettler, Life in the "plastisphere": microbial communities on plastic marine debris, *Environ. Sci. Technol.*, 2013, **47**, 7137–7146.
4 H.-C. Flemming and J. Wingender, The biofilm matrix, *Nat. Rev. Microbiol.*, 2010, **8**, 623–633.
5 M. Arias-Andres, U. Klümper, K. Rojas-Jimenez and H.-P. Grossart, Microplastic pollution increases gene exchange in aquatic ecosystems, *Environ. Pollut.*, 2018, **237**, 253–261.
6 J. S. Madsen, M. Burmølle, L. H. Hansen and S. J. Sørensen, The interconnection between biofilm formation and horizontal gene transfer, *FEMS Immunol. Med. Microbiol.*, 2012, **65**, 183–195.
7 G. Bhardwaj, M. Abdulkadhim, K. Joshi, L. Wankhede, R. K. Das and S. K. Brar, Exposure Pathways, Systemic Distribution, and Health Implications of Micro- and Nanoplastics in Humans, *Appl. Sci.*, 2025, **15**, 8813.
8 X. Wu, J. Pan, M. Li, Y. Li, M. Bartlam and Y. Wang, Selective enrichment of bacterial pathogens by microplastic biofilm, *Water Res.*, 2019, **165**, 114979.
9 G. Bhardwaj, L. Wankhede, R. Pulicharla and S. K. Brar, Microplastic-associated biofilms in wastewater treatment plants: Mechanisms and impacts, *J. Water Proc. Eng.*, 2025, **72**, 107582.
10 S. Oberbeckmann, B. Kreikemeyer and M. Labrenz, Environmental Factors Support the Formation of Specific Bacterial Assemblages on Microplastics, *Front. Microbiol.*, 2017, **8**, 2709.
11 K. Parrish and N. L. Fahrenfeld, Microplastic biofilm in fresh- and wastewater as a function of microparticle type and size class, *Environ. Sci.: Water Res. Technol.*, 2019, **5**, 495–505.
12 S. Rajcoomar, I. D. Amoah, T. Abunama, N. Mohlomi, F. Bux and S. Kumari, Biofilm formation on microplastics in wastewater: insights into factors, diversity and inactivation strategies, *Int. J. Sci. Environ. Technol.*, 2024, **21**, 4429–4444.
13 G. Bhardwaj, M. Mohammadiun, C. S. Osorio Gonzalez, S. Kaur Brar and S. Karimpour, Wastewater-induced microplastic biofouling in freshwater: role of particle size and flow velocity, *Environ. Sci. Adv.*, 2025, **4**, 90–96.
14 M. Zarean, S. H. Dave, S. K. Brar and R. W. M. Kwong, Environmental drivers of antibiotic resistance: Synergistic effects of climate change, co-pollutants, and microplastics, *J. Hazard. Mater. Adv.*, 2025, **19**, 100768.
15 C. Li, L. Wang, S. Ji, M. Chang, L. Wang, Y. Gan and J. Liu, The ecology of the plastisphere: Microbial composition, function, assembly, and network in the freshwater and seawater ecosystems, *Water Res.*, 2021, **202**, 117428.
16 S. Oberbeckmann and M. Labrenz, Marine Microbial Assemblages on Microplastics: Diversity, Adaptation, and Role in Degradation, *Ann. Rev. Mar. Sci.*, 2020, **12**, 209–232.
17 F. Murphy, C. Ewins, F. Carbonnier and B. Quinn, Wastewater Treatment Works (WwTW) as a Source of Microplastics in the Aquatic Environment, *Environ. Sci. Technol.*, 2016, **50**, 5800–5808.
18 X. Li, L. Chen, Q. Mei, B. Dong, X. Dai, G. Ding and E. Y. Zeng, Microplastics in sewage sludge from the wastewater treatment plants in China, *Water Res.*, 2018, **142**, 75–85.

19 S. Huang, B. Zhang, Z. Zhao, C. Yang, B. Zhang, F. Cui, P. N. L. Lens and W. Shi, Metagenomic analysis reveals the responses of microbial communities and nitrogen metabolic pathways to polystyrene micro(nano)plastics in activated sludge systems, *Water Res.*, 2023, **241**, 120161.
20 B. Zhang, S. Huang, L. Wu, Y. Guo, W. Shi and P. N. L. Lens, Micro(nano)plastic size and concentration co-differentiate the treatment performance and toxicity mechanism in aerobic granular sludge systems, *Chem. Eng. J.*, 2023, **457**, 141212.
21 Q. Li, L. Tian, X. Cai, Y. Wang and Y. Mao, Plastisphere showing unique microbiome and resistome different from activated sludge, *Sci. Total Environ.*, 2022, **851**, 158330.
22 Y. Feng, J.-W. Sun, W.-W. Shi, J.-L. Duan, X.-D. Sun, L.-J. Feng, Q. Wang, Y.-D. Gan and X.-Z. Yuan, Microplastics exhibit accumulation and horizontal transfer of antibiotic resistance genes, *J. Environ. Manage.*, 2023, **336**, 117632.
23 L. Shen, Y. Wang, R. Liu, Y. Yang, Y. Liu and B. Xing, Aging characteristics of degradable and non-biodegradable microplastics and their adsorption mechanism for sulfonamides, *Sci. Total Environ.*, 2023, **901**, 166452.
24 S. Martínez-Campos, M. González-Pleiter, F. Fernández-Piñas, R. Rosal and F. Leganés, Early and differential bacterial colonization on microplastics deployed into the effluents of wastewater treatment plants, *Sci. Total Environ.*, 2021, **757**, 143832.
25 G. Bhardwaj, R. K. Das, A. Eldyasti, A. Koubaa and S. K. Brar, Differential impacts of conventional and biodegradable microplastics on treatment performance and bacterial community in sequencing batch reactors, *Bioresour. Technol. Rep.*, 2025, **32**, 102344.
26 K. Yang, Q.-L. Chen, M.-L. Chen, H.-Z. Li, H. Liao, Q. Pu, Y.-G. Zhu and L. Cui, Temporal Dynamics of Antibiotic Resistome in the Plastisphere during Microbial Colonization, *Environ. Sci. Technol.*, 2020, **54**, 11322–11332.
27 D. Lobelle and M. Cunliffe, Early microbial biofilm formation on marine plastic debris, *Mar. Pollut. Bull.*, 2011, **62**, 197–200.
28 B. J. Callahan, P. J. McMurdie, M. J. Rosen, A. W. Han, A. J. A. Johnson and S. P. Holmes, DADA2: High-resolution sample inference from Illumina amplicon data, *Nat. Methods*, 2016, **13**, 581–583.
29 Y. Lu, G. Zhou, J. Ewald, Z. Pang, T. Shiri and J. Xia, MicrobiomeAnalyst 2.0: comprehensive statistical, functional and integrative analysis of microbiome data, *Nucleic Acids Res.*, 2023, **51**, W310–W318.
30 Y. Wang, X. Liu, C. Huang, W. Han, P. Gu, R. Jing and Q. Yang, Antibiotic resistance genes and virulence factors in the plastisphere in wastewater treatment plant effluent: Health risk quantification and driving mechanism interpretation, *Water Res.*, 2025, **271**, 122896.
31 K. P. Lai, C. F. Tsang, L. Li, R. M. K. Yu and R. Y. C. Kong, Microplastics act as a carrier for wastewater-borne pathogenic bacteria in sewage, *Chemosphere*, 2022, **301**, 134692.
32 M. Ogonowski, A. Motiei, K. Ininbergs, E. Hell, Z. Gerdes, K. I. Udekwu, Z. Bacsik and E. Gorokhova, Evidence for selective bacterial community structuring on microplastics, *Environ. Microbiol.*, 2018, **20**, 2796–2808.
33 D. K. Tuyen, S. Jeong, K. Cho and H.-T. Nguyen, Biological treatment shaping microplastic-associated microbial communities in wastewater treatment plant, *J. Water Proc. Eng.*, 2025, **76**, 108120.
34 X. Guo, Y.-R. Chen, X. Sun, C. Li, L. Hou, M. Liu and Y. Yang, Plastic properties affect the composition of prokaryotic and eukaryotic communities and further regulate the ARGs in their surface biofilms, *Sci. Total Environ.*, 2022, **839**, 156362.
35 J.-W. Lee, J.-H. Nam, Y.-H. Kim, K.-H. Lee and D.-H. Lee, Bacterial communities in the initial stage of marine biofilm formation on artificial surfaces, *J. Microbiol.*, 2008, **46**, 174–182.
36 L. Miao, P. Wang, J. Hou, Y. Yao, Z. Liu, S. Liu and T. Li, Distinct community structure and microbial functions of biofilms colonizing microplastics, *Sci. Total Environ.*, 2019, **650**, 2395–2402.
37 J. J. Kelly, M. G. London, A. R. McCormick, M. Rojas, J. W. Scott and T. J. Hoellein, Wastewater treatment alters microbial colonization of microplastics, *PLoS One*, 2021, **16**, e0244443.
38 F. Bydalek, G. Webster, R. Barden, A. J. Weightman, B. Kasprzyk-Hordern and J. Wenk, Microplastic biofilm, associated pathogen and antimicrobial resistance dynamics through a wastewater treatment process incorporating a constructed wetland, *Water Res.*, 2023, **235**, 119936.
39 R. A. Wilkes, N. Zhou, A. L. Carroll, O. Aryal, K. P. Teitel, R. S. Wilson, L. Zhang, A. Kapoor, E. Castaneda, A. M. Guss, J. R. Waldbauer and L. Aristilde, Mechanisms of Polyethylene Terephthalate Pellet Fragmentation into Nanoplastics and Assimilable Carbons by Wastewater Comamonas, *Environ. Sci. Technol.*, 2024, **58**, 19338–19352.
40 Y. Jiao, A. Zhou, D. Zhang, M. Chen and L. Wan, Distinct microbial community structures formed on the biofilms of PLA and PP, influenced by physicochemical factors of sediment and polymer types in a 60-day indoor study, *Front. Environ. Sci.*, 2024, **12**, 1452523.
41 D. N. Pham, L. Clark and M. Li, Microplastics as hubs enriching antibiotic-resistant bacteria and pathogens in municipal activated sludge, *J. Hazard. Mater. Lett.*, 2021, **2**, 100014.
42 S. Y. Kim, S. Woo, S.-W. Lee, E.-M. Jung and E.-H. Lee, Dose-Dependent Responses of Escherichia coli and Acinetobacter sp. to Micron-Sized Polystyrene Microplastics, *J. Microbiol. Biotechnol.*, 2025, **35**, 1–10.
43 A. S. Tagg, T. Sperlea, M. Labrenz, J. P. Harrison, J. J. Ojeda and M. Sapp, Year-Long Microbial Succession on Microplastics in Wastewater: Chaotic Dynamics Outweigh Preferential Growth, *Microorganisms*, 2022, **10**, 1775.
44 M. I. Love, W. Huber and S. Anders, Moderated estimation of fold change and dispersion for RNA-seq data with DESeq2, *Genome Biol.*, 2014, **15**, 550.

45 D. M. P. De Oliveira, B. M. Forde, T. J. Kidd, P. N. A. Harris, M. A. Schembri, S. A. Beatson, D. L. Paterson and M. J. Walker, Antimicrobial Resistance in ESKAPE Pathogens, *Clin. Microbiol. Rev.*, 2020, **33**, e00181-19.
46 A. Pękala-Safińska, Contemporary threats of bacterial infections in freshwater fish, *J. Vet. Res.*, 2018, **62**, 261–267.
47 S. Jia and X. Zhang, in *High-Risk Pollutants in Wastewater*, ed. H. Ren and X. Zhang, Elsevier, 2020, pp. 41–78.
48 M. Shen, Z. Zeng, L. Li, B. Song, C. Zhou, G. Zeng, Y. Zhang and R. Xiao, Microplastics act as an important protective umbrella for bacteria during water/wastewater disinfection, *J. Clean. Prod.*, 2021, **315**, 128188.
49 J. Brandon, M. Goldstein and M. D. Ohman, Long-term aging and degradation of microplastic particles: Comparing in situ oceanic and experimental weathering patterns, *Mar. Pollut. Bull.*, 2016, **110**, 299–308.
50 S. Monira, R. Roychand, F. I. Hai, M. Bhuiyan and B. K. Pramanik, Microplastic fragmentation into nanoplastics by water shear forces during wastewater treatment: Mechanical insights and theoretical analysis, *Environ. Pollut.*, 2025, **364**, 125310.